Validation Studies of Gyrokinetic Turbulence Simulations Via Multi-scale and Multi-field Turbulence Measurements on the DIII-D Tokamak

T.L. Rhodes 1), C.H. Holland 2), S.P. Smith 3), A.E. White 4), K.H. Burrell 3), J. Candy 3), J.C. DeBoo 3), E.J. Doyle 1), J.C. Hillesheim 1), J.E. Kinsey 3), G.R. McKee 5), D. Mikkelsen 6), W.A. Peebles 1), C.C. Petty 3), R. Prater 3), S. Parker 7), Y. Chen 7), L. Schmitz 1), G.M. Staebler 3), R.E. Waltz 3), G. Wang 1), Z. Yan 5), and L. Zeng 1)

1) Physics Dept. and PSTI, University of California, Los Angeles, California 90095, USA
2) University of California San Diego, San Diego, 92093-0417 USA
3) General Atomics, P.O. Box 85608, San Diego, California 92186-5608, USA
4) Massachusetts Institute of Technology, Boston, Massachusetts, USA
5) University of Wisconsin-Madison, Madison, Wisconsin, USA
6) Princeton Plasma Physics Laboratory, Princeton, New Jersey, USA
7) Center for Integrated Plasma Studies, University of Colorado, Colorado, USA

e-mail contact of main author: trhodes@ucla.edu

Abstract. A series of carefully designed experiments on DIII-D have taken advantage of a broad set of turbulence and profile diagnostics to rigorously test gyrokinetic turbulence simulations. In this paper the goals, tools, and experiments performed in these validation studies are reviewed and specific examples presented. It is found that predictions of transport and fluctuation levels in the mid-core region ($0.4<\rho<0.75$) are in better agreement with experiment than those in the outer region ($\rho\geq0.75$) where edge coupling effects may become increasingly important and multi-scale simulations may also be necessary. Validation studies such as these are crucial in developing confidence in a first-principles based predictive capability for ITER.

1. Introduction

First principles predictive simulation of plasma confinement and performance is one of the over-arching goals of fusion research today [1,2]. Numerous experiments, measurements, and simulation codes from across the world are focused on this goal. A series of carefully designed experiments on DIII-D have taken advantage of a broad set of turbulence and profile diagnostics to address this 'grand challenge'. In this paper the goals, tools, and experiments performed in these validation studies are reviewed and specific examples presented. Although still in the early days, this effort has found that predictions of transport and fluctuation levels in the mid-core region ($0.4<\rho<0.75$) are often in better agreement with experiment than those in the outer region ($\rho\geq0.75$). One explanation of this is the increasing importance of edge effects as the plasma boundary is approached. Results such as these are noteworthy as they point to significant research paths. Validation studies are crucial in developing confidence in a first-principles based predictive capability for ITER and other, future burning plasma experiments.

Validation studies are defined as that process which compares measurements to simulated values in order to assess the underlying physics modeling accuracy of the simulation. A related branch of study is that termed 'verification' which deals with the question of whether a simulation accurately solves the equations upon which it is based. Verification does not address whether the underlying equations adequately represent the real world. Thus a simulation may be verified as correctly solving the equations contained within it but it may fail validation if it does not adequately predict relevant measurements. The present study deals only with validation questions and therefore assumes that the codes have been adequately verified [e.g. see Refs. [3–5] and references therein for further discussions relating to these two different endeavors].

The question of what constitutes agreement (or alternatively disagreement) arises early in the process. For these purposes, agreement is defined to occur when the predicted values lie within the uncertainties of the measured values. Complexity quickly arises as agreement often occurs in one set of parameters while significant disagreement is seen in others (e.g. agreement between measured and predicted electron thermal energy fluxes but disagreement between experiment and simulations for the ion thermal energy flux). Various complex measures or metrics have been proposed that deal with this issue which address multiple parameters, radii, and uncertainties [5]. However, these metrics are outside the scope of the present paper.

Given that experimental measurements are the foundation of this work, it is extremely useful to obtain multiple measures of the same or similar quantities to cross compare for potential bias and error. For example, on DIII-D two measurements of density and electron temperature are obtained via Thomson scattering, electron cyclotron emission (ECE), and reflectometry. In the case of a diagnostic failure, a second measure is invaluable. In addition, errors and bias are potentially resolvable via multiple measurements and in the case of disagreement the experimentalist is alerted to potential issues. Typical validation experiments involve multiple repeat discharges and/or plasma 'jogs' (small rigid body shifts of the plasma) to both scan the fluctuation diagnostics as well as to obtain multiple measures of the background density, temperature, safety factor, etc. profiles for statistical analysis. These repeat shots and profiles are used to quantify the profile uncertainty and to provide some insight into uncertainties in the resulting transport calculations. Figure 1 diagrams this comparison process. The process is fairly straightforward and natural, however it is worth pointing out the red horizontal arrow marked 'profiles, flux surface shape, …'. This is the necessary experimental input to the simulations, thus the predictions are only as good as these inputs and any uncertainties should be propagated through in order to provide an accurate determination of the validity of the comparison.

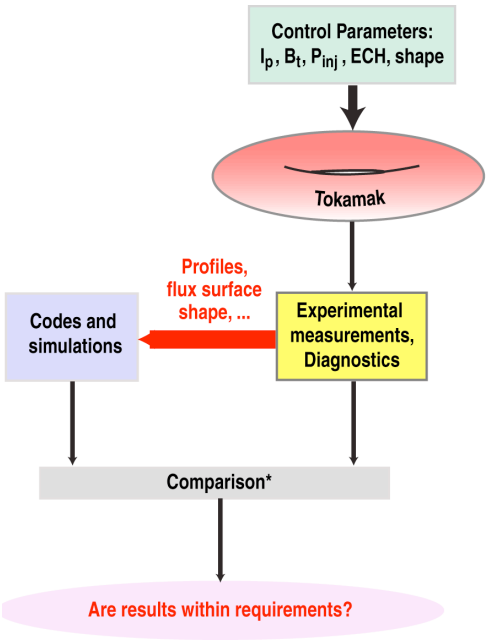

FIG. 1. Validation procedure highlighting experimental input to the simulations.

First principles based simulations predict transport levels due to simulated turbulence induced transport. For this reason, validation studies are focused upon comparisons of both fundamental level fluctuation parameters (amplitudes, cross-phases, spectra, etc.) and higher level transport quantities (e.g. thermal and particle fluxes). Comparisons of thermal and particle fluxes require that the simulated fluxes include the same components included in the experimental fluxes (e.g. convected and conducted terms). Arguably greater care must be taken to accurately compare turbulence measurements to simulation values. Fluctuation measurements have specific wavenumber, frequency, and spatial ranges and resolutions that must be accurately represented when comparing to simulation data. For example, it is insufficient to extract electron temperature fluctuations from a non-linear simulation and compare it directly to a correlation ECE measurement of $\tilde{T}_e$. The simulation data must be analyzed in a manner analogous to the measurement technique, taking into account wavenumber, time, and spatial resolutions, as well as any particular measurement nuances such as cross correlation of multiple spatial volumes (as is done with CECE $\tilde{T}_e$). The codes used in this type of analysis are

termed synthetic diagnostics. Specific examples and full descriptions of synthetic diagnostics used at DIII-D can be found in Refs. [6,7].

In the next section, the approach used by validation studies at DIII-D is described followed by an overview of the experimental and simulation tools utilized and validation experiments performed at DIII-D. A detailed examination of a recent T_e/T_i scan L-mode experiment is then provided along with non-linear calculations and comparisons. A summary and conclusion follows.

2. Approach to Validation Studies

The validation studies approach at DIII-D is two-fold, addressing both qualitative and quantitative aspects of comparisons. The simulations should at the very least replicate the qualitative variations while deviations at the quantitative level can shed light on the underlying physics model limitations. Typically a single plasma variable is chosen with the choice based upon a known and ideally strong response. Examples of such variables are plasma elongation (κ), safety factor (q), electron to ion temperature ratio T_e/T_i, gradients in T_e and T_i, etc. A strong plasma response facilitates these studies by providing clear changes for comparison and also by raising the results out of naturally occurring noise and fluctuation levels. These qualitative/quantitative variations include radial variations as well as changes due to the just discussed parametric variations. Figure 2 uses data from a plasma elongation (κ) experiment conducted on DIII-D to illustrate this qualitative/quantitative approach. Plasma elongation is a useful parameter due to its known strong effect on plasma confinement in tokamaks [8]. The figure shows turbulent electron temperature fluctuations over the frequency range 0–200 kHz for two plasma elongation shapes, κ=1.4 and 1.1. The fluctuation levels are significantly larger for the low κ shape. In addition, it was found that the energy confinement is also lower for the lower κ shape. For this example, a simulation prediction that has high fidelity (defined here as the degree to which the simulation accurately reproduces experiment) will predict both the qualitative variation of $\tilde{T}_e$ with κ and the qualitative increase of $\tilde{T}_e$ with radius as well as the quantitative values. Note that in validation studies, comparisons are made with as large a range of measurements as possible (discussed further in the next section). In so doing, the study seeks to reveal aspects of the simulation code that require further investigation.

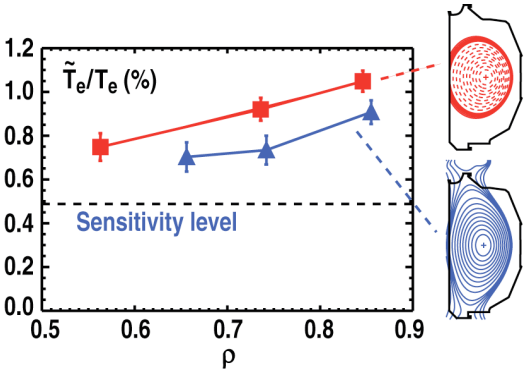

FIG. 2. Demonstrating experimental change in radial $\tilde{T}_e$ profile due to change in plasma elongation.

3. Tools Available at DIII-D

The DIII-D tokamak has a significant number of profile and fluctuation diagnostics available for validation studies. Profile diagnostics include charge exchange recombination (CER) for T_i, impurity density, toroidal and poloidal rotation, and electric field profiles; motional Stark effect (MSE) for core safety factor profiles; Thomson scattering for T_e and n_e; electron cyclotron emission for T_e; and reflectometry for n_e profiles. Fluctuation diagnostics include beam emission spectroscopy (BES) for low-k $\tilde{n}$ and turbulence flows, Doppler backscattering (DBS) for turbulence flows and intermediate-k $\tilde{n}$, millimeter wave backscattering for high-k $\tilde{n}$, correlation ECE for low-k electron temperature fluctuations $\tilde{T}_e$, and phase contrast imaging (PCI) for low through intermediate-k $\tilde{n}$. These diagnostics have differing operational requirements as well as differing wavenumber, spatial, and temporal resolutions. The individual diagnostic requirements and limitations must be accounted for in the design of the experiment as well as in the design of the synthetic diagnostic used to interpret the simulation

predictions. The available diagnostics are diagrammatically related to various instability wavenumbers of interest in Fig. 3. This figure shows wavenumber ranges and available measurements. For example, in the trapped electron mode (TEM) wavenumber range both PCI and DBS make measurements. Other overlapping measurements include BES and reflectometry for low-k $\tilde{n}$. As with multiple measures of equilibrium parameters (e.g. ECE and Thomson scattering for T_e) these provide checks and verifications of the fluctuation measurements. Recently added measurements include local, wavenumber resolved TEM scale $\tilde{n}$, fluctuating turbulence flows, and density-temperature (n_eT_e) turbulence cross-phase. The novel measurement of the n_eT_e crossphase is important in gyrokinetic validation studies since it represents the relationship between different fluctuating fields – density and temperature (it is also closely related to the cross-phase that determines the turbulent transport) and since it can be directly compared to simulation at a fundamental level. The unique array of multi-field, multi-scale turbulence measurements has been utilized to study a wide range of target plasmas with excellent spatial coverage (the typical radial range of these studies is r/a~0.55–0.85 although a larger range is possible).

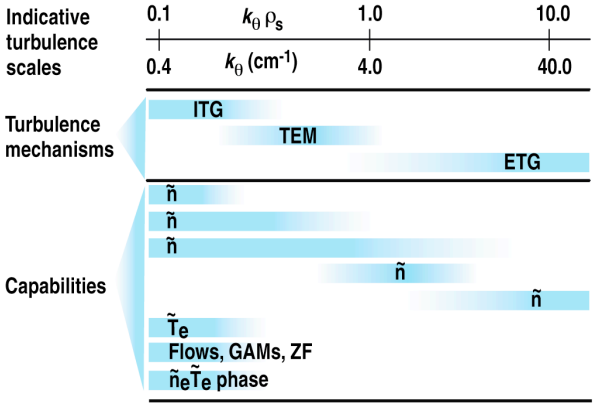

r/a	Δr (cm)	System
-1–1	60	(FIR)
0.25–1$^+$	1	(BES,reflct)
0.4–1	1–10	(PCI)
0–1$^+$	1	(DBS)
0–1$^+$	1, 20	(DBS, HKBS)
0–0.9	1	(CECE, ECEI)
0–1$^+$	1	(BES,DBS)
0–0.9	1	(DBS/CECE)

FIG. 3 Multi-field and multi-scale fluctuation diagnostics on DIII-D. Comparing wavenumber ranges of representative instabilities to diagnostic wavenumber range. Diagnostic system, measurement, approximate spatial coverage, and spatial resolutions are indicated.

The DIII-D tokamak is a medium sized tokamak, with major radius R~1.7 m, minor radius a~0.6 m, magnetic field B=0.6–2.1T, plasma current 1–2 MA, elongation κ~1–2, ~17.5 MW neutral beam injection, ~3.5 MW electron cyclotron heating, and ≤3.6 MW fast wave heating. Plasma shaping and control are very flexible with a large range in size, triangularity, elongation, etc. possible. This parameter range, shaping flexibility, heating choices, and broad diagnostic coverage combine to make DIII-D an excellent choice for validation studies.

Validation studies are focused on the testing and validation of a wide range of gyrokinetic turbulence codes/simulations. The simulation code most extensively utilized to-date is GYRO [9] and more recently GENE [10], GEM [11], GTC [12], and GYSELA [13] have begun to enter the process. To date the most complete simulations of DIII-D validation experiments has been performed by GYRO. GYRO is a physically comprehensive nonlinear gyrokinetic code containing: ion temperature gradient (ITG) physics, trapped and passing electrons, electron-ion pitch angle collisions, electromagnetic effects, *ExB* and parallel flow shears, real geometry, *ExB* and magnetic flutter transport. GYRO and GEM can be run in either a local flux tube or a global simulation mode. Here flux tube generally means that the gradients of interest (L_n, L_{Ti}, etc.) do not vary across the simulation domain whereas in a global simulation they are allowed to vary.

4. Experiments Performed

A series of plasma experiments were performed for validation studies at DIII-D. The target plasmas are selected to address plasma parameters that have a large plasma response such

that both experiment and simulation show significant variations. Table 1 illustrates the range of plasma parameters addressed, percentage parameter variation achieved, and the plasma confinement regime utilized. Note that the largest variations achieved are of order 50% with some as small as 25%. Planned future studies include scans of safety factor q and collisionality. In the next section the results from the L-mode T_e/T_i scan experiment shown in Table 1 is examined in detail and compared to simulation.

Table 1. Parameters Utilized and Variation Achieved in Validation Studies at DIII-D

Parameter	Variation	Plasma
Elongation, κ	30%	L-mode [14]
T_e/T_i	30%	L-mode [this paper]
T_e/T_i	25%	Hybrid H-mode
T_e/T_i	50%	QH-mode [15]
Local L_{Te}	50%	L-mode [16]
$\tilde{n}_e$–$\tilde{T}_e$ cross phase	50%	L-mode [17]

5. L-mode T_e/T_i scan experimental measurements and comparison to simulation

Plasma Description. The effect of varying T_e/T_i in an L-mode, diverted plasma was examined by applying ECH heating to an NBI heated plasma. The base case was a sawtooth-free upper single null plasma, chord averaged density n_{avg} = 2.3x10^{19} m^{-3}, toroidal magnetic field B_T = 2.05 T, plasma current I_p = 1 MA, and neutral beam power P_{NBI} = 2.5 MW. T_e was increased via approximately 3.3 MW of electron cyclotron heating applied near radial location ρ=0.2. The experimental goal was to keep the other plasma parameters of interest as similar as possible, with the exception of the desired change in T_e/T_i, between the two cases. Figure 4 shows profiles of interest for the two cases, lower T_e (heated by Ohmic and NBI only), and higher T_e (Ohmic, NBI, and ECH). An increase is observed in the electron temperature with some variation in the other parameters as well. The radial range of interest for these validation studies is ρ=0.5-0.8. In this range the ratio T_e/T_i is seen to increase by ~30% in the radial range ρ=0.5-0.8, with the largest variation in other parameters occurring in the inverse ion temperature scale length a/L_{Ti} and collisionality. Changes in these parameters affect the stability calculations for the various instabilities of interest (e.g. ITG, TEM, ETG instabilities) and must be accounted for. Although it is preferred and simpler if only one parameter is varied, the plasma simulations will take into account all measured changes allowing a consistent comparison. The decrease in a/L_{Ti} with ECH will generally result in lower ITG growth rates while the decrease in collisionality with ECH will result in higher TEM growth rates. The situation in a real plasma, where the various instabilities are coupled via the background plasma, can be more complicated.

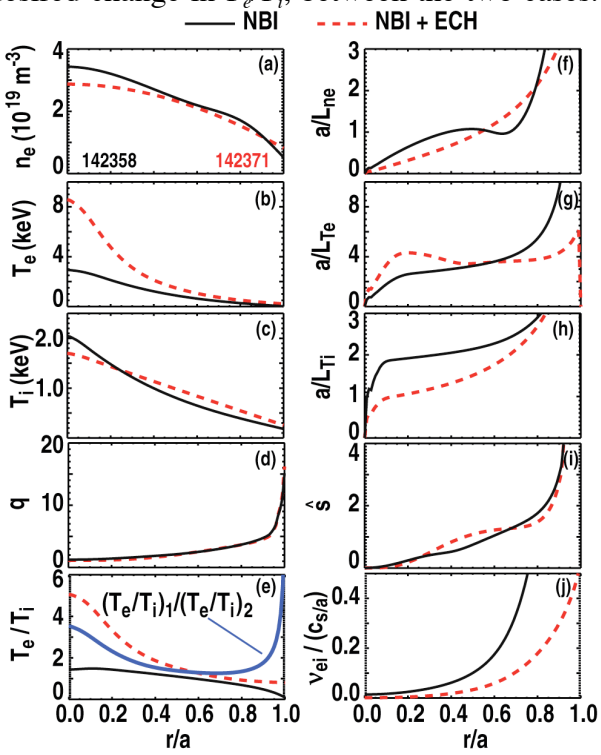

FIG. 4 Experimental radial profiles of (a) n_e, (b) T_e, (c) T_i, (d) q, (e) T_e/T_i ratio, and normalized inverse scale lengths (f) a/L_{ne}, (g) a/L_{Te}, (h) a/L_{Ti}, (i) magnetic shear s=dlnq/dlnr, (j) collisionality, ν_{ei}/C_s. Here a is the minor radius on the midplane, and c_s is the ion sound velocity. NBI and NBI + ECH cases shown.

Fluctuation Measurements. Electron temperature fluctuations ($\tilde{T}_e$ from CECE) showed the largest response to the additional ECH. Profiles of electron temperature fluctuations covering the radial range ρ=0.5-0.8 are shown in Fig. 5(a). The normalized fluctuation levels are typical of the core of L-mode plasmas being in the range 0.5 to 3%. The fluctuation level increases by as much as 70% with ECH. In contrast, the low-k density fluctuations (from BES) showed little or no response within the error bars, [Fig. 5(b)]. Radial profiles of intermediate-k density fluctuations (from DBS) show no discernable change with ECH [Fig. 5(c)]. Examination of wavenumber spectra of these intermediate-k $\tilde{n}$ (k~3.5–6 cm^{-1}, from DBS) at ρ=0.55 (not shown) show some signs of redistribution of power in k space however the levels remain roughly unchanged. High-k density fluctuations ($k \sim 35$ cm^{-1}) from millimeter wave backscattering (not shown) indicate little change with ECH. Figure 6 summarizes the observed changes in fluctuations due to the additional ECH. Interestingly, the temperature fluctuations have a much stronger response as compared to the density fluctuations.

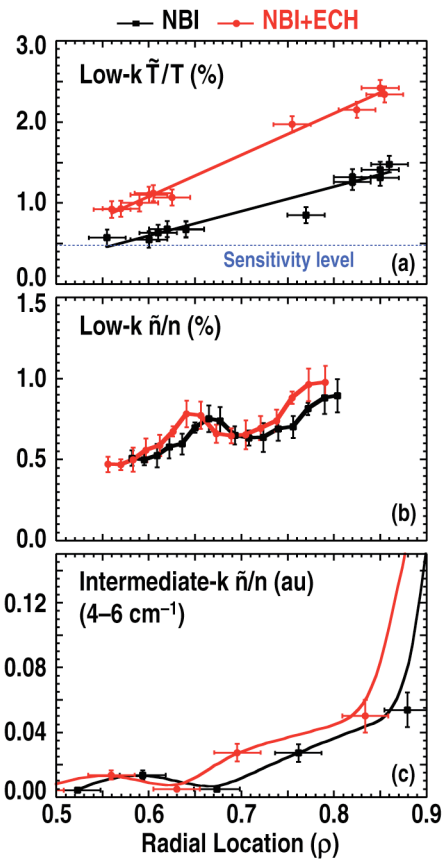

FIG. 5. Experimental radial profiles of (a) low-k $\tilde{T}_e$ (CECE), (b)low-k $\tilde{n}$ (BES), and (c) intermediate-k $\tilde{n}$ (DBS) for NBI only and NBI + ECH cases.

Non-linear Gyrokinetic Predictions. The nonlinear GYRO code [18] was used to examine the fluctuations and transport at ρ=0.6 for the two plasma conditions shown in Fig. 4. Flux-tube runs were performed resolving wavenumbers $k_\theta \rho_s \leq 1.1$, where ρ_s=0.21 cm and 0.25 for NBI and NBI + ECH cases respectively. The measured ExB shear was included in the simulations. The runs were electromagnetic, with mass ratio $(M_{ion}/m_e)^{1/2}$=40, where m_e is the electron mass and M_i is the main ion (deuterium) mass. A single impurity (carbon) species was included in the calculations. Electrons are drift kinetic so that the effect of finite electron Larmor radius was excluded. Figure 7 shows predicted electron temperature and electron density fluctuations for the two cases. Note that the figure shows power spectra vs. wavenumber normalized to the local T_e and n values respectively. For reference and comparison to experiment, the predicted normalized RMS fluctuation levels after preliminary processing of the spectra via synthetic diagnostics is indicated in Fig. 7. It is seen that the predicted temperature fluctuations increase with ECH by a factor of ~2.6, from 0.86% to 2.2%, and the predicted $\tilde{n}/n$ increases by a factor of ~1.15 from 0.41% to 0.47%. The predicted low-k $\tilde{T}_e/T$ variation is qualitatively similar to the experimental variation but differs quantitatively while the predicted low-k $\tilde{n}/n$ variation appears to differ qualitatively from experiment. The simulation of $\tilde{n}/n$ at higher wavenumbers is underway.

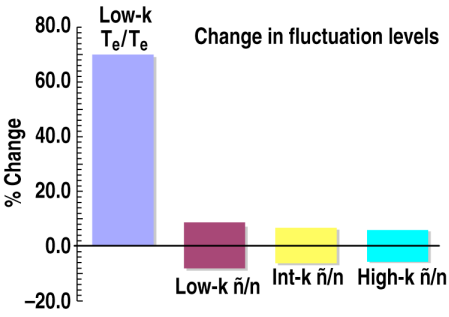

Fig. 6. Summary of changes in experimental fluctuations comparing NBI and NBI+ECH cases. Radial location ρ=0.6.

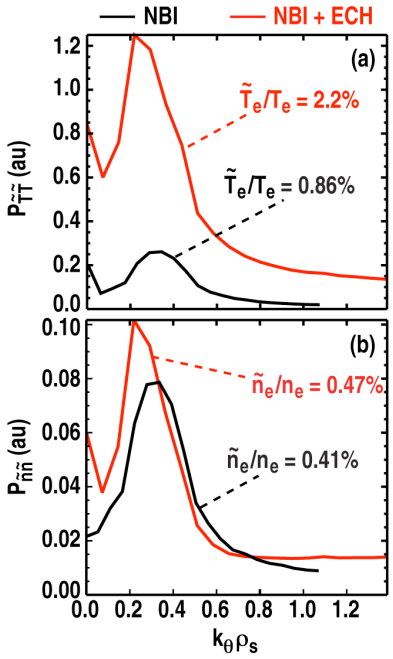

FIG. 7. GYRO simulated power spectra for (a) $\tilde{T}_e$ and (b) electron $\tilde{n}$. NBI and NBI + ECH cases.

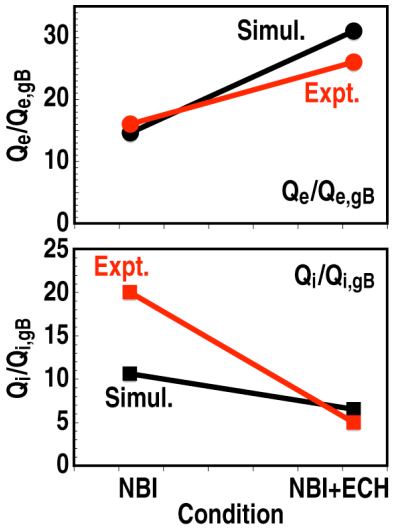

FIG. 8. Simulation and experiment (a) electron and (b) ion thermal fluxes at ρ=0.6 normalized to gyro-Bohm flux, $Q_{eB} = n_e c_s T_e$. NBI and NBI + ECH cases.

Figure 8 shows a comparison of the ion and electron thermal fluxes (normalized to the gyro-Bohm flux at that radius, $Q_{gB} = n_e c_s T_e$) at ρ=0.6 from experiment and simulation. The normalization by $Q_{gB} \sim T_e^{3/2}$ obscures the amount of increase in absolute Q_e with ECH (also note that absolute Q_i increases with ECH, whereas the normalized quantity decreases due to the $Q_{gB} \sim T_e^{3/2}$ variation). The fluxes are plotted vs. the nominal plasma condition and show similar qualitative behavior between the experimental and predicted values. The quantitative values for the electron fluxes also compare favorably. In contrast the quantitative ion fluxes for the NBI case differ by a factor of two between simulation and prediction while being similar for the NBI+ECH case. Note that these simulations use the profiles shown in Fig. 4 with no attempt at thermal flux matching or profile variation. These flux matching and variation studies are underway and some improvement in the agreement may occur.

Non-linear GYRO simulations were attempted for radial location ρ=0.8. However, physically meaningful solutions have not been obtained to date at this location, with the simulations exhibiting an unphysical accumulation of fluctuation energy at the highest simulation wavenumbers ($k_\theta \rho_s \sim 1$. to 1.5). This phenomenon is known to correlate with strong intermediate to high-k growth rates, suggesting a need for multiscale simulations (e.g. coupled ITG-TEM-ETG) and is currently under further investigation. The radial location where this effect begins to manifest itself is also of importance and studies are underway to determine this as well.

These observations fit a general trend for validation studies at DIII-D in that predictions of transport and fluctuation levels in the mid-core region ($0.4<\rho<0.75$) are often in better agreement with experiment than those in the outer region ($\rho>0.75$) [6,14,16,17,19]. As a further illustration, Fig. 9 shows experimental profiles and simulations from shot 128913, an L-mode shot used extensively in validation studies [6,16]. The integrated energy flows through the local surface area (P_e and P_i) from both a transport model

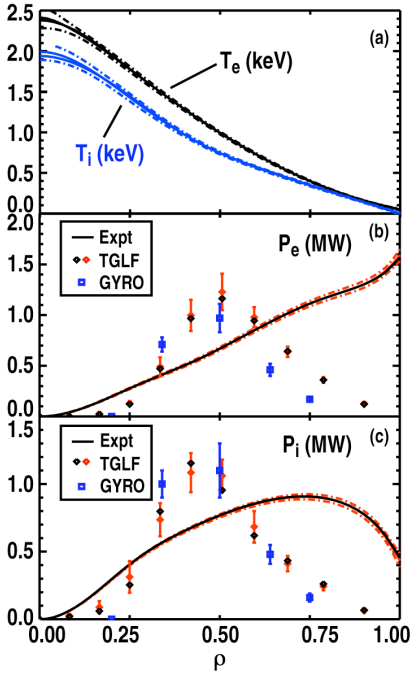

Fig. 9 (a) Experimental T_e, T_i, (b) experimental and predicted electron energy flow through the local surface area (P_e), (c) experimental and predicted ion energy flow through the local surface area (P_i).

(TGLF [20]) and non-linear GYRO show qualitative and some quantitative similarity to experiment in the radial range $\rho<0.6$. However, as ρ increases, significant under prediction of the fluxes [Fig. 9(c,d)] begins near $\rho=0.6$ and approaches a 50% or larger under prediction near $\rho=0.7$ and beyond. These flows are based on the experimental profiles shown in Fig. 9(a). These observations indicate a possible research path that addresses this edge under-prediction in a systematic way.

8. Summary

Validation studies on DIII-D are focused on the testing of a wide range of gyrokinetic turbulence codes/simulations. Through this ongoing validation activity, where experimental measurement is compared in detail with simulation prediction, the design of suitably rigorous experiments for testing code predictions has steadily improved. An example of this process was described where it was found that predictions of temperature fluctuation levels and transport fluxes are in qualitative agreement with experiment at $\rho=0.6$ but were not obtainable at $\rho=0.8$. Further investigations of this are underway. These observations appear similar to other observations from validation studies on DIII-D where predictions of transport and fluctuation levels in the mid-core region ($0.4<\rho<0.75$) are in better agreement with experiment than those in the outer region ($\rho>0.75$) where edge coupling effects may become increasingly important and multi-scale simulations may also be necessary.

Acknowledgment

Work supported by U.S. DOE under DE-FG02-08ER54984, DE-FC02-04ER54698, DE-FG02-95ER54309, DE-FC02-93ER54186, DE-FG02-07ER54917, DE-FG02-89ER54296, DE-FG02-08ER54999 and DE-AC02-09CH11466.

References

[1] DAWSON, John M. , et al., Intl. J. High Performance Computing Applic. **5**, 13 (1991).
[2] TANG, W. M., Phys. Plasmas **9**, 1856 (2002).
[3] ROACHE, P.J., *Verification and Validation in Computational Science and Engineering*, Hermosa Publishers, Albuquerque (1998).
[4] OBERKAMP, William L., and TRUCANO, Timothy G., Nucl. Engin. Design **238**, 716 (2008).
[5] TERRY, P.W., et al., Phys. Plasmas **15**, 062503 (2008).
[6] HOLLAND, C., et al., Phys. Plasmas **16**, 052301 (2009).
[7] WHITE, A.E., et al. Phys. Plasmas 17, 056103 (2010).
[8] PETTY, C.C., Phys. Plasmas **15**, 080501 (2008).
[9] CANDY, J., and WALTZ, R.E., J. Comput. Phys. **186**, 545 (2003).
[10] JENKO, F., DORLAND, W. and HAMMETT, G.W., Phys. Plasmas **8**, 4096 (2001).
[11] CHEN, Y., and PARKER, S.E., J. Comput. Phys. **220**, 839 (2007).
[12] LIN, Z., et al., Science **281**, 1835 (1998).
[13] GRANDGIRARD, V., et al., Plasma Phys. Control. Fusion **49**, B173 (2007).
[14] HOLLAND, C., personal communication, also to be presented at the APS 2010 meeting.
[15] SCHMITZ, L., et al., "Reduced Electron Thermal Transport in Low Collisionality H-mode Plasmas in DIII-D and the Importance of Small-Scale Turbulence," these proceedings, EXC/P7-01 .
[16] DEBOO, J. C. ,et al., Phys. Plasmas **17**, 056105 (2010).
[17] WHITE, A. E. ,et al., Phys. Plasmas **17**, 056103 (2010).
[18] CANDY, J., and WALTZ, R.E., J. Comput. Phys. **186**, 545 (2003).
[19] WHITE, A.E., et al., PHYSICS OF PLASMAS **15**, 056116 (2008).
[20] KINSEY, J.E., et al., PHYSICS OF PLASMAS **15**, 055908 (2008).